

Multi-field Return Point Memory

Nathaniel Croce

Department of Mechanical Engineering and Materials Science, Duke University, Durham, NC, 27708, USA

Hossein Salahshoor

Department of Civil and Environmental Engineering, Duke University, Durham, NC, 27708, USA
Department of Mechanical Engineering and Materials Science, Duke University, Durham, NC, 27708, USA

D. Zeb Rocklin

School of Physics, Georgia Institute of Technology, Atlanta, GA 30332

(Dated: May 25, 2026)

Non-equilibrium systems display memory, a dependence not merely on their present environment but on previously applied fields. Multistable systems such as spin glasses, martensites and granular matter have exponentially many microstates consistent with an applied field, making their rich dynamics difficult to control. Control and order can be achieved through the concept of partial ordering, which we here generalize to systems subject to multiple control fields. We demonstrate, within the model system of the zero-temperature Ising model, that this leads to return-point memory, in which an applied sequence of fields restores the hysteretic system not only to a previous magnetization, but to a previous exact microstate. The multiplicity of fields grants more precise and complex control of the system, with different classes of operations displaying commutative and noncommutative behavior. This grants new insight into how physical systems can remember, learn, and be trained.

Physical systems in equilibrium have many commonalities, including the laws of thermodynamics, detailed balance, fluctuation-dissipation theorems and observable physical values derived from phase-space averaging [1]. Nonequilibrium systems, by contrast, exhibit a much broader range of behaviors, but far fewer universal organizing principles. One of the most important such behaviors is memory, which refers to the ability of a system to encode information about previously applied perturbations in its present state and future response [2, 3]. Memory formation has been observed across a wide range of driven and disordered systems, including charge-density waves [4, 5], granular materials [6], suspensions and disordered solids [7–12], structural and spin glasses [13–15], and active matter [16]. More broadly, memory is central to function in biological systems [17, 18], and newly emerging physical learning in tunable mechanical networks [19–25]. These examples suggest that memory converts a disordered or multistable material from a passive medium into an information-bearing physical system.

Among the many forms of material memory, return-point memory occupies a special place because it is exact and reproducible. In a system with return-point memory, a bounded excursion of an applied field returns the system not only to a previous macroscopic observable, but to a previous microscopic state. The canonical theoretical setting is the zero-temperature random-field Ising model driven by a single scalar field, where ferromagnetic interactions, metastable relaxation, partial ordering, and the no-passing property imply nested hysteresis loops and exact return to prior states [26–29]. This framework has shaped our understanding of disorder-driven hysteresis and avalanches in magnets, martensites, and other irre-

versible systems [30]. However, the classical theory relies crucially on a scalar driving where histories can be ordered by their maxima and minima along a single field. Yet, many programmable and mechanical systems of current interest are controlled by more than one independent input, such as multiple forces, displacements, stresses, strains, actuation patterns, fields, or boundary motions. In such systems, the applied drive is a path in a multidimensional control space, and there is no natural total ordering of histories. This raises a basic question: can return-point memory survive under multi-field or vector-valued driving, and if so, what replaces the scalar ordering structure that makes the classical theory work?

In this Letter, we introduce the multi-field random-field Ising model as a minimal setting for addressing this question. Each spin is coupled ferromagnetically to its neighbors and experiences quenched disorder, but the external drive consists of multiple independently controlled fields acting on different spatial patterns of spins. We show that monotone paths in this multidimensional control space lead to the same final microstate, independent of the particular path taken. For non-monotone paths, however, distinct field operations generally do not commute: applying the same changes in different orders can lead to different final microstates. Despite this noncommutativity, we prove and demonstrate a multi-field form of return-point memory in which bounded variations in control space exactly restore the system to an earlier microstate. This extends return-point memory from scalar hysteresis loops to multidimensional protocols and suggests new principles for organizing, retrieving, and transforming microstates in trainable multistable matter.

We consider a system based on the Ising model [31],

which has seen widespread application in statistical physics [32, 33] consisting of a square grid (periodic boundary conditions are assumed) of spins, each of which can be either up (+1) or down (-1), as shown in Fig. 1 (a) and the associated Supplementary Video. We retain the Ising model's original language of magnetic spins and fields, but the same model has been effectively applied beyond standard statistical physics systems to neurons [34], buckling beams [35] and curving surfaces [36, 37]. We term our model the multi-field Ising model (MFIM), and define it by the following energy functional:

$$E = -J \sum_{\langle i,j \rangle} s_i s_j - \sum_i \left(h_i^0 + \sum_a c_a(t) H_{ai} \right) s_i. \quad (1)$$

Here, $J > 0$ is a coupling constant between each spin and its four neighbors and h_i^0 is a quenched (static) field that is different at different sites, where we typically take h_i^0 to be independently and identically normally distributed with mean zero and standard deviation σ . We introduce the concept of multiple *control fields* $c_a(t)$ which each undergo some prescribed evolution under time t . The coefficients $H_{ai} \geq 0$ describe how strong a field control a exerts on site i . Note that the total energy can be expressed in the form $E = -\sum_i h_i s_i$, where the local field h_i is a combination of interactions, quenched disorder and the control fields.

Appropriate for macroscale systems, we take our system to be at zero temperature, meaning that after a change in the external fields, spins flip to lower the energy, eventually reaching a local minimum in the multi-stable energy landscape induced by disorder. As shown in the Supplementary Material [SM (IV)], the order in which spins flip does not affect the final state. We can define a *partial ordering* on the system states, such that one state is greater than or equal to another if each spin in the first state is greater than or equal to the corresponding spin in the second state. While the vast majority of pairs of microstates are not ordered in this sense, the states obey a *no-passing condition*, in which two ordered states maintain their order when subjected to the same fields. This type of condition was first identified for sliding charge-density waves [26] and later extended to spin systems [27].

The special case of only a single field that applies equally to all spins ($H_{1i} = \text{const.}$) has been extensively studied and referred to as the random-field Ising model (RFIM) [27, 28, 38, 39]. In this Letter, we mainly focus on the case of checkerboard fields, in which one field is applied to all even sites (in which their horizontal and vertical indices sum to an even integer) and another field is applied to all odd sites, as shown in Fig. 1 (b), although we also include an example of many-field control. In the particular control protocol shown in Fig. 1 (c), the field on the even sites (in units such that $J = 1$) is ramped up,

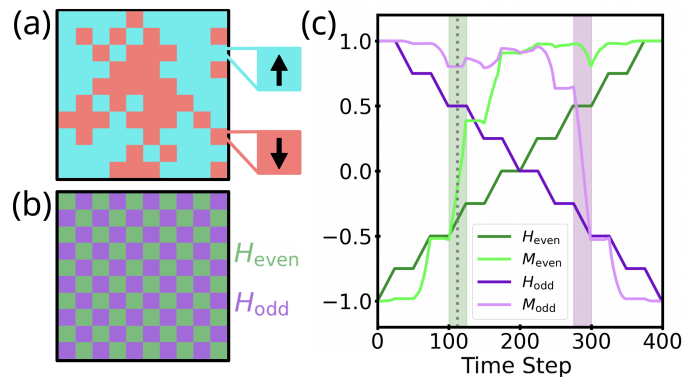


FIG. 1. **Application and behavior of system with two external fields.** (a) An arbitrary snapshot of a 10×10 subset of a 100×100 spin configuration at time $t = 112$: light blue squares represent a positive spin at the site (+1) and light red squares represent a negative spin (-1). (b) The H_{even} (green) and H_{odd} (purple) fields are applied in a checkerboard pattern across the 10×10 lattice of spins. (c) Time evolution of the external fields H_{even} (dark green) and H_{odd} (dark purple) over time, and the corresponding magnetization at the even sites M_{even} (light green) and the odd sites M_{odd} (light purple) when H_{even} and H_{odd} are applied to a 100×100 lattice of spins in the checkerboard pattern demonstrated in (b). The shaded region corresponds to instances where one of the two H fields are held constant. Dashed-line corresponds to arbitrary time step $t = 112$.

resulting in some of the spins to which this field is applied flipping up. This in turn can flip some of the other spins up, so that both even and odd magnetizations (defined as the average values of the corresponding spins) increase. In other time steps, the odd field is decreased, resulting in both even and odd spins flipping down, so that the overall magnetization is roughly maintained while shifting from odd to even magnetization.

In a separate protocol depicted in Fig. 2 (a) (magenta line), we begin in a state with zero field applied, increase the first field, and then subsequently increase the second field. As spins flip to align with the external fields and each other, the system passes through microstates labeled I, II and IV as shown in Fig. 2 (b) (see also the associated Supplementary Video). Separately, we consider a protocol (yellow line) in which the increase in the odd field occurs before the increase in the even field. While the system passes through a different set of intermediate states, such as III, than in the previous protocol, it arrives at exactly the same final state (IV). This is a demonstration of the more general phenomenon of *equivalence of monotonic paths*. That is, as proven in the Supplementary Material [SM (VI)], when an initial state is subject to an initial set of fields at some time t_0 and evolved monotonically under changing fields to some final state at time t_f , the result depends on the initial state and the initial and final fields, but is independent of the particular monotonic path. Here, we say that a path is monotonically increasing only if for ev-

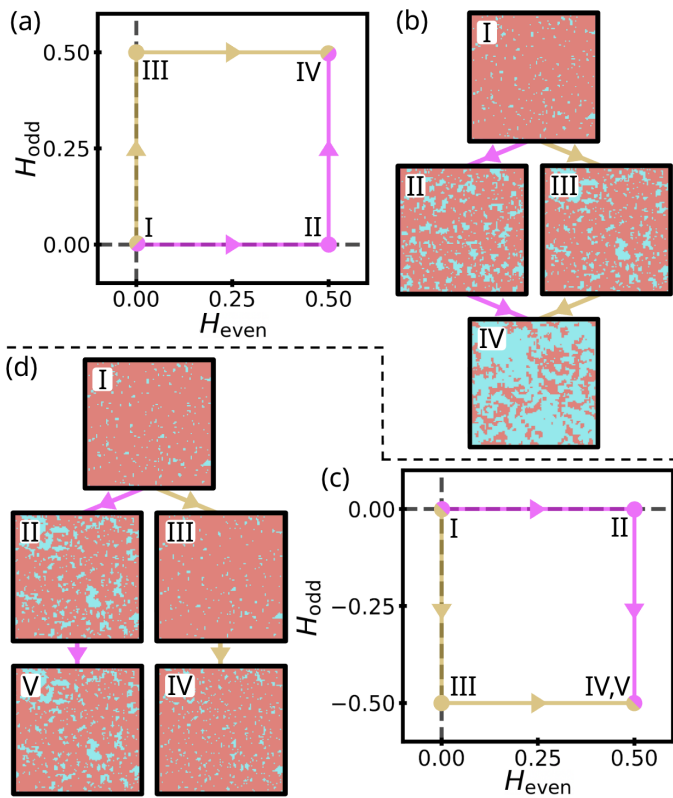


FIG. 2. **Commutativity and non-commutativity in a two field system.** (a) Two systems begin from identical initial configurations (I) and evolve under distinct monotonic fields trajectories in the $(H_{\text{even}}, H_{\text{odd}})$ plane. Path 1 (pink) first increases H_{even} , and then increases H_{odd} , while Path 2 (yellow) reverses the order. Because both field components vary monotonically and reach the same final values, the resulting final configurations are identical (IV) as depicted in (b). The intermediate configurations (II,III) differ and exhibit no relation. (c) depicts a similar setup to (a) starting with two identical systems, but they now evolve under distinct non-monotonic field trajectories. Path 1 (pink) first increases H_{even} , and then decreases H_{odd} , while Path 2 (yellow) reverses the order. Although both paths terminate at the same external field values, their final spin configurations (V,IV) differ as depicted in (d). Notably, V is greater than IV because Path 1 begins with an increase while Path 2 begins with a decrease; for the same reason, II is greater than III.

ery $t_0 \leq t_1 \leq t_2 \leq t_f$ that $h_i(t_1) \leq h_i(t_2)$ for each site i . Given our positive coefficients H_{ai} , this is ensured so long as each control field $c_a(t)$ is increasing. Unlike the single-field result [27], this equivalence is over an infinite number of monotonic paths through control space. Because increasing fields can be applied to different sites in any order, these actions can be interpreted as commuting operators acting on the system, akin to the abelian nature [40] of the sandpile model [41].

We also consider non-monotonic paths, such as the two protocols shown in Fig. 2(c). In the first protocol (magenta) the even field is increased and then the odd

field is decreased. In the second protocol (yellow) the order of these operations is reversed, so that the system follows a different path in field space to the same final applied fields. In contrast with the strictly increasing paths, not only are the respective intermediate states shown in Fig. 2(d) (II, III) different, the final states (V, IV) differ as well (see also the associated Supplementary Video). Furthermore, we can say that the protocol in which the field increase occurs earlier generates a final state that is greater than or equal to (in the partial ordering sense) the state resulting from the protocol in which the field decrease occurs earlier, as shown in the Supplementary Material [SM (VII)]. This sensitivity to the order of the applied fields demonstrates the general *non-commutativity* of non-monotonic control fields. Non-commutativity is a hallmark of history-dependent systems, and is essential to performing logical operations and achieving robotic control in multistable systems [42].

In general, a multistable system might have many different states consistent with an applied field, as is the case for frustrated antiferromagnets and spin glasses [15]. Consequently, when the applied fields are evolved over time in a closed loop, it is not generally the case that the system state will similarly return to its initial microstate. However, as shown in the Supplementary Material [SM (IX)], the independence of bounded paths (ones in which the applied fields remain within a given range of values), leading to a novel form of *return-point memory* [3, 27, 30], in which the return to the exact microstate, among hundreds or thousands of stable states that exist at these fields, is achieved. This can be seen in Fig. 3(a), in which both fields are gradually increased, passing through state I, before reaching a maximum value, at which point the system reaches state II. The two control fields are then reduced independently. At an intermediate timestep, they reach the same external control fields, but the resulting state, III, lies strictly above state I, with many spins flipped. This is a form of hysteresis, in which the same applied fields result in different states due to history-dependence. However, as the fields are separately restored to their maximum values, the system is likewise restored to its same microstate, IV, which is identical to state II. The distinction is that between states II and IV, the applied fields remained bounded, lying between the maximum associated with state II and the minimum at initialization—in contrast, between states I and III, the applied fields increased to new maxima. In Fig. 3(b), the protocol is repeated with 10,000 different fields, one applied to each spin, taken through a random path in field space (only ten are depicted in the graph). Despite the extreme complexity of the protocol, the system is likewise restored to the exact microstate when the fields are brought back to their maximum values, as also shown in the accompanying Supplementary Video.

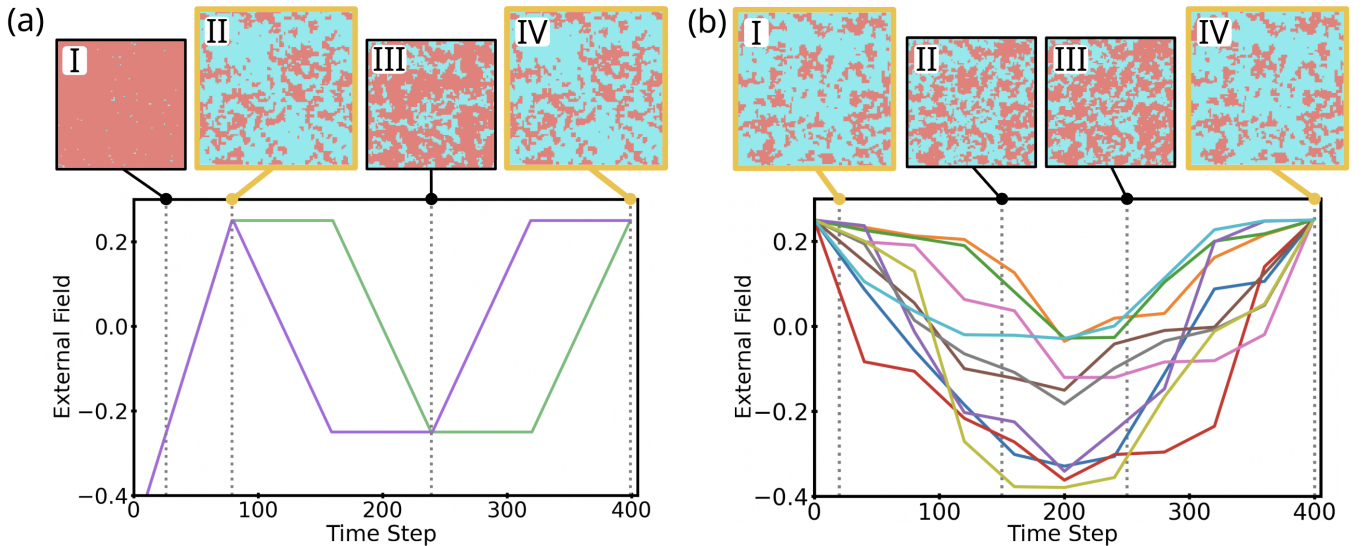


FIG. 3. **Demonstration of return point memory in two-field and multi-field system.** (a) The external fields H_{even} (green) and H_{odd} (purple) fields evolve over time as shown. Both fields begin at large negative values and rapidly increase to pass through spin configuration I and reach spin configuration II. The fields then vary independently over time until reconverging to produce final configuration IV, which is identical to state II. Notice that H_{even} and H_{odd} never exceed the extrema reached during state I, consistent with the no-passing rule, and thus states II and III are less than I. (b) 100×100 external fields evolve over time (only 10 fields are depicted on the plot) and are applied to a 100×100 spin lattice, allowing each field to act on only a single spin. The spin configurations exhibit the same return point memory effect demonstrated in (a).

In Fig. 4(a), a two-field protocol is shown in which the fields are ramped up to their maximum values separately, before spiraling up and down through a range of values. Because of the spiral nature of the field path, ramping up the fields results in returning three separate times to previous field strengths (purple dots). As shown in Fig. 4(b), this results in returning to the exact same microstates and hence magnetizations (purple dots). Fig. 4(c) shows the relationship between one of the applied fields and the magnetizations in the same path, as also depicted in the associated Supplementary Video.

We have shown how physical systems subject to complex controls display return-point memory. This enhanced control raises the possibility of developing new applications of the effect, such as proposed magnetic memory systems [43], of training the systems to desired response profiles, or realizing the effect at other length scales or via other types of interactions. Extending the proof of return-point memory, we also advance the possibility of explaining the effect in other systems in which it has been reported, such as antiferromagnets [29, 44].

Acknowledgments We gratefully acknowledge financial support from the National Science Foundation CAREER program (#2338492), from the Army Research Office through the MURI program (#W911NF2210219) and through NSF PHY2309135 to the Kavli Institute for Theoretical Physics (KITP) (DZR).

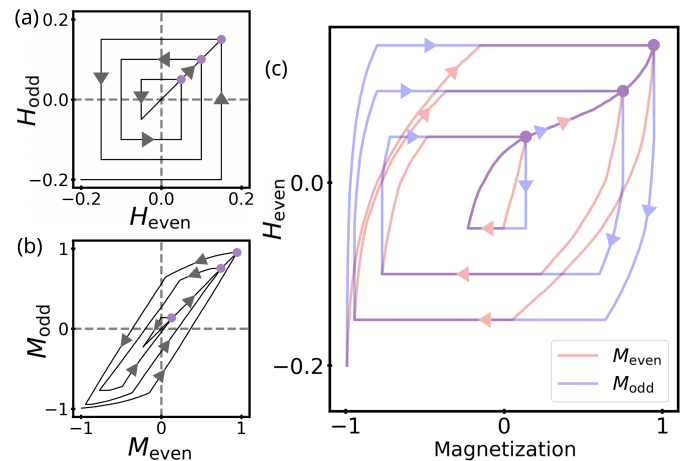


FIG. 4. **Repeated return-point memory effect via spiral control dynamics.** (a) A 200×200 spin system evolves under a spiral trajectory plotted in the $(H_{\text{even}}, H_{\text{odd}})$ plane. (b) A resulting similar behaving spiral occurs as the system evolves when plotting the magnetization at the even sites and odd sites of the system in the $(M_{\text{even}}, M_{\text{odd}})$ plane. (c) The behavior of M_{even} and M_{odd} are each demonstrated individually when plotted against H_{even} . The three purple points demonstrate instances of return point memory in the system between when the path first intersects a point during the inward spiral and when the point is intersected again during the final increase. Each instance of return point memory in (c) also has a corresponding instance in the $(H_{\text{even}}, H_{\text{odd}})$ plane in (a) and the $(M_{\text{even}}, M_{\text{odd}})$ plane in (b).

Codes The computer code used for the generation of data, as well as the videos can be accessed at <https://github.com/natepcroce/MultiField-RPM>.

-
- [1] R. K. Pathria, *Statistical Mechanics: International Series of Monographs in Natural Philosophy*, Vol. 45 (Elsevier, 2017).
- [2] N. C. Keim, J. D. Paulsen, Z. Zeravcic, S. Sastry, and S. R. Nagel, Memory formation in matter, *Reviews of Modern Physics* **91**, 035002 (2019).
- [3] J. D. Paulsen and N. C. Keim, Mechanical memories in solids, from disorder to design, *Annual Review of Condensed Matter Physics* **16**, 61 (2025).
- [4] S. N. Coppersmith and P. B. Littlewood, Pulse-duration memory effect and deformable charge-density waves, *Physical Review B* **36**, 311 (1987).
- [5] S. N. Coppersmith, T. C. Jones, L. P. Kadanoff, A. Levine, S. R. Nagel, and S. C. Venkataramani, Self-organized short-term memories, *Physical Review Letters* **78**, 3983 (1997).
- [6] C. Jossierand, A. V. Tkachenko, D. M. Mueth, and H. M. Jaeger, Memory effects in granular materials, *Physical Review Letters* **85**, 3632 (2000).
- [7] N. C. Keim and S. R. Nagel, Generic transient memory formation in disordered systems with noise, *Physical Review Letters* **107**, 010603 (2011).
- [8] J. D. Paulsen, N. C. Keim, and S. R. Nagel, Multiple transient memories in experiments on sheared non-brownian suspensions, *Physical Review Letters* **113**, 068301 (2014).
- [9] Y. Lahini, O. Gottesman, A. Amir, and S. M. Rubinstein, Nonmonotonic aging and memory retention in disordered mechanical systems, *Physical Review Letters* **118**, 085501 (2017).
- [10] S. Dillavou and S. M. Rubinstein, Nonmonotonic aging and memory in a frictional interface, *Physical Review Letters* **120**, 224101 (2018).
- [11] N. C. Keim and D. Medina, Mechanical annealing and memories in a disordered solid, *Science Advances* **8**, eabo1614 (2022).
- [12] D. Shohat and Y. Lahini, Dissipation indicates memory formation in driven disordered solids, *Physical Review Letters* **130**, 048202 (2023).
- [13] D. Fiocco, G. Foffi, and S. Sastry, Encoding of memory in sheared amorphous solids, *Physical Review Letters* **112**, 025702 (2014).
- [14] S. Mukherji, N. Kandula, A. K. Sood, and R. Ganapathy, Strength of mechanical memories is maximal at the yield point of a soft glass, *Physical Review Letters* **122**, 158001 (2019).
- [15] K. Binder and A. P. Young, Spin glasses: Experimental facts, theoretical concepts, and open questions, *Reviews of Modern Physics* **58**, 801 (1986).
- [16] M. C. Marchetti, J.-F. Joanny, S. Ramaswamy, T. B. Liverpool, J. Prost, M. Rao, and R. A. Simha, Hydrodynamics of soft active matter, *Reviews of modern physics* **85**, 1143 (2013).
- [17] J. J. Hopfield, Neural networks and physical systems with emergent collective computational abilities, *Proceedings of the National Academy of Sciences* **79**, 2554 (1982).
- [18] D. J. Amit, H. Gutfreund, and H. Sompolinsky, Spin-glass models of neural networks, *Physical Review A* **32**, 1007 (1985).
- [19] M. Stern, M. B. Pinson, and A. Murugan, Continual learning of multiple memories in mechanical networks, *Physical Review X* **10**, 031044 (2020).
- [20] M. Stern, D. Hexner, J. W. Rocks, and A. J. Liu, Supervised learning in physical networks: From machine learning to learning machines, *Physical Review X* **11**, 021045 (2021).
- [21] S. Dillavou, M. Stern, A. J. Liu, and D. J. Durian, Demonstration of decentralized physics-driven learning, *Physical Review Applied* **18**, 014040 (2022).
- [22] S. Dillavou, B. D. Beyer, M. Stern, A. J. Liu, M. Z. Miskin, and D. J. Durian, Machine learning without a processor: Emergent learning in a nonlinear analog network, *Proceedings of the National Academy of Sciences* **121**, e2319718121 (2024).
- [23] M. Stern and A. Murugan, Learning without neurons in physical systems, *Annual Review of Condensed Matter Physics* **14**, 417 (2023).
- [24] S. Li and X. Mao, Training all-mechanical neural networks for task learning through in situ backpropagation, *Nature communications* **15**, 10528 (2024).
- [25] R. Mandal, R. Huang, M. Fruchart, P. G. Moerman, S. Vaikuntanathan, A. Murugan, and V. Vitelli, Learning dynamical behaviors in physical systems, *arXiv preprint arXiv:2406.07856* (2024).
- [26] A. A. Middleton, Asymptotic uniqueness of the sliding state for charge-density waves, *Physical review letters* **68**, 670 (1992).
- [27] J. P. Sethna, K. Dahmen, S. Kartha, J. A. Krumhansl, B. W. Roberts, and J. D. Shore, Hysteresis and hierarchies: Dynamics of disorder-driven first-order phase transformations, *Physical Review Letters* **70**, 3347 (1993).
- [28] J. P. Sethna, K. A. Dahmen, and O. Perkovic, Random-field ising models of hysteresis, in *The Science of Hysteresis* (Elsevier, 2006) pp. 107–179.
- [29] J. M. Deutsch, A. Dhar, and O. Narayan, Return to return point memory, *Physical Review Letters* **92**, 227203 (2004).
- [30] J. P. Sethna, M. K. Bierbaum, K. A. Dahmen, C. P. Goodrich, J. R. Greer, L. X. Hayden, J. P. Kent-Dobias, E. D. Lee, D. B. Liarte, X. Ni, *et al.*, Deformation of crystals: Connections with statistical physics, *Annual Review of Materials Research* **47**, 217 (2017).
- [31] E. Ising, Beitrag zur theorie des ferromagnetismus, *Zeitschrift für Physik* **31**, 253 (1925).
- [32] J. P. Sethna, *Statistical mechanics: entropy, order parameters, and complexity*, Vol. 14 (Oxford University Press, 2021).
- [33] J. Cardy, *Scaling and renormalization in statistical physics*, Vol. 5 (Cambridge university press, 1996).
- [34] Y. Roudi, J. Tyrcha, and J. Hertz, Ising model for neural data: model quality and approximate methods for extracting functional connectivity, *Physical Review E—Statistical, Nonlinear, and Soft Matter Physics* **79**, 051915 (2009).
- [35] S. H. Kang, S. Shan, A. Košmrlj, W. L. Noorduin, S. Shian, J. C. Weaver, D. R. Clarke, and K. Bertoldi, Complex ordered patterns in mechanical instability induced geometrically frustrated triangular cellular structures, *Physical review letters* **112**, 098701 (2014).

- [36] A. Plummer and D. R. Nelson, Buckling and metastability in membranes with dilation arrays, *Physical Review E* **102**, 033002 (2020).
- [37] A. Plummer, P. Z. Hanakata, and D. R. Nelson, Curvature as an external field in mechanical antiferromagnets, *Physical Review Materials* **6**, 115203 (2022).
- [38] N. G. Fytas, V. Martín-Mayor, M. Picco, and N. Surlas, Review of recent developments in the random-field ising model, *Journal of Statistical Physics* **172**, 665 (2018).
- [39] D. Belanger and A. Young, The random field ising model, *Journal of magnetism and magnetic materials* **100**, 272 (1991).
- [40] D. Dhar, Self-organized critical state of sandpile automaton models, *Physical Review Letters* **64**, 1613 (1990).
- [41] P. Bak, C. Tang, and K. Wiesenfeld, Self-organized criticality: An explanation of the $1/f$ noise, *Physical review letters* **59**, 381 (1987).
- [42] T. Zhao, X. Dang, K. Manos, S. Zang, J. Mandal, M. Chen, and G. H. Paulino, Modular chiral origami metamaterials, *Nature* **640**, 931 (2025).
- [43] O. Perković and J. P. Sethna, Improved magnetic information storage using return-point memory, *Journal of applied physics* **81**, 1590 (1997).
- [44] D. Shohat, D. Hexner, and Y. Lahini, Memory from coupled instabilities in unfolded crumpled sheets, *Proceedings of the National Academy of Sciences* **119**, e2200028119 (2022).